Application of the three omega thermal conductivity measurement method to a film on a substrate of finite thickness

Jung Hun Kim, Albert Feldman, and Donald Novotny

Citation: Journal of Applied Physics **86**, 3959 (1999);
View online: https://doi.org/10.1063/1.371314
View Table of Contents: http://aip.scitation.org/toc/jap/86/7
Published by the American Institute of Physics

Application of the three omega thermal conductivity measurement method to a film on a substrate of finite thickness

Jung Hun Kim,[a] Albert Feldman, and Donald Novotny
National Institute of Science and Technology, Gaithersburg, Maryland 20899

(Received 10 May 1999; accepted for publication 23 June 1999)

The three omega thermal conductivity measurement method is analyzed for the case of one or more thin films on a substrate of finite thickness. The analysis is used to obtain the thermal conductivities of SiO_2 films on Si substrates and of a chemical vapor deposition (CVD) diamond plate. For the case of the SiO_2 films on a Si, we find an apparent thickness dependence of the thermal conductivity of the SiO_2 films. However, the data can also be explained by a thickness-independent thermal conductivity and an interfacial thermal resistance. For the case of the CVD diamond plate, the fit of the theory to the experimental data is significantly improved if we assume that an interface layer separates the heater from the diamond plate. [S0021-8979(99)01319-5]

I. INTRODUCTION

The three omega thermal conductivity measurement method has been used extensively to measure the thermal properties of bulk and thin film dielectric materials.[1–4] A detailed description of the experimental method we have used for measuring thermal conductivity (κ) has been given by D. G. Cahill.[5] The method employs a metallic strip in intimate contact with the specimen surface. An ac electrical current modulated at angular frequency ω is induced to flow in the strip causing heat generation in the strip. The heating has both a dc component which changes the average temperature of the specimen and an ac component at 2ω which generates thermal waves in the specimen. Because the electrical resistance of the strip depends on the temperature, the resistance will be modulated at 2ω as well. Therefore, there will be an ac voltage drop across the ends of the strip at 3ω, $V_{3\omega}$, which is proportional to the ac temperature variation of the strip at 2ω, $T_{2\omega}$. $T_{2\omega}$ will depend on the thermal conductivity, κ, of each underlying material. Thus, it is possible to extract κ from a measurement of $V_{3\omega}$ vs ω. In the case of a thin film on a thick substrate, $V_{3\omega}$ will usually depend linearly on $\ln(\omega)$ in which case the data are relatively simple to analyze. However, if the thermal diffusion length in the substrate is greater than the thickness of the substrate, then $V_{3\omega}$ will deviate from a linear dependence on $\ln(\omega)$ because of thermal wave reflections from the back surface of the substrate. In this case, one must perform a nonlinear least squares analysis based on a more exact model in order to extract κ.

In this article, we present the solution to the three omega thermal conductivity measurement method for several films on a substrate of finite thickness. Based on a nonlinear least squares fit of the solution to experimental data, we have calculated κ of silicon dioxide films on silicon substrates (SiO_2/Si films) and κ of a diamond plate which is assumed to be separated from the metal heating strip by a thin interface layer. In the former case, we also obtain values for κ of Si which are a little smaller than handbook values.

In the context of this article, a ''thick'' layer refers to a layer that is considered to be infinitely thick because the layer thickness is much greater than the longest thermal diffusion length being considered.

II. TWO-DIMENSIONAL MULTILAYER HEAT FLOW

Consider a multilayer system in vacuum with the layers numbered from bottom to top from 1 to n. The heater is in contact with the top surface of the top layer, layer n. The 3ω signal is obtained from the ac temperature of the top surface of the top layer. Figure 1 shows cross sections of the sample geometries evaluated; the geometry is two-dimensional. An ac current at ω flows through the heater strip normal to the plane of page, generating heat at 2ω. We can generalize D. G. Cahill's expression[1] for the ac surface temperature for a multilayer system averaged over the strip, thus

$$\Delta T = \frac{P}{2\pi l b^2} \times \int_0^\infty \frac{B^+(m)+B^-(m)}{A^+(m)B^-(m)-A^-(m)B^+(m)} \frac{\sin^2(mb)}{\gamma_n m^2}\, dm, \tag{1}$$

where

$$\gamma_j = \kappa_j \sqrt{m^2 - i\frac{\omega}{D_j}}, \tag{2}$$

where the subscript $j=n$ refers to the nth layer which is located just beneath the heater strip, P is amplitude of the ac power generated in the heater strip, l is the length of the heater strip, b is the width of the heater strip, m is the variable of integration, κ_j is the thermal conductivity of layer j, D_j is the thermal diffusivity of layer j, and $A^+(m)$, $A^-(m)$, $B^+(m)$, $B^-(m)$ are parameters determined by a matrix

[a]Guest scientist from the Korea Research Institute of Standards and Science.

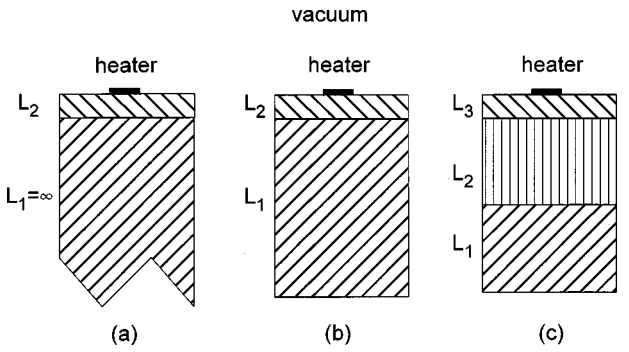

FIG. 1. The schematic diagram of the material configurations used to model the three omega thermal conductivity measurement method. (a) Film on a semi-infinite substrate (offset model). (b) Film on a substrate of finite thickness (two-layer model). (c) Three-layer model.

procedure[6] analogous to that given in H. S. Carslaw and J. C. Jaeger.[7] In this article, we have modified the nomenclature given in Ref. 6 by reversing the numbering of the layers. This allows us to use a simple recursion relationship that relates a system with $n+1$ layers to a system with n layers. The recursion relations show symbolically how $B^+(m)$ and $B^-(m)$ change if we add a layer, thus

$$\begin{pmatrix} B^+ \\ B^- \end{pmatrix}_{n+1} = \frac{1}{2\gamma_{n+1}} \begin{pmatrix} e^{-u_{n+1}L_{n+1}} & 0 \\ 0 & e^{u_{n+1}L_{n+1}} \end{pmatrix} \times \begin{pmatrix} \gamma_{n+1}+\gamma_n & \gamma_{n+1}-\gamma_n \\ \gamma_{n+1}-\gamma_n & \gamma_{n+1}+\gamma_n \end{pmatrix} \begin{pmatrix} B^+ \\ B^- \end{pmatrix}_n, \tag{3}$$

where,

$$u_j = \sqrt{m^2 - i\frac{\omega}{D_j}}, \tag{4}$$

where L_j is the thickness of layer j, and the dependence of all other parameters on m is implied. The subscripts on the **B** vectors denote the number of layers being considered. Regardless of the number of layers, $A^+(m)=1/2$ and $A^-(m)=1/2$. When $n=0$, $B^+(m)=0$ and $B^-(m)=1$.

Although the procedure in Ref. 6 is one-dimensional, the same procedure is applicable, with appropriate substitutions, to the particular fourier component of the temperature considered in this case. This is because the boundary conditions in both cases lead to the same equations.

As an example, we give the values of $B^+(m)$ and $B^-(m)$ for case *b* of Fig. 1

$$\begin{pmatrix} B^+ \\ B^- \end{pmatrix}_2 = \begin{pmatrix} \frac{1}{4\gamma_2}[(\gamma_2+\gamma_1)e^{-u_1L_1}+(\gamma_2-\gamma_1)e^{u_1L_1}]e^{-u_2L_2} \\ \frac{1}{4\gamma_2}[(\gamma_2-\gamma_1)e^{-u_1L_1}+(\gamma_2+\gamma_1)e^{u_1L_1}]e^{-u_2L_2} \end{pmatrix}. \tag{5}$$

Case *c* is obtained by an additional application of Eq. (3).

III. SPECIMENS

Table I lists the specimen specifications. The SiO_2 films were produced on silicon wafers by the steam/dry oxidation method and the thicknesses were measured by ellipsometry. The estimated relative standard uncertainty in the film thickness measurement is 1%.

The diamond specimen had been part of a previously reported set of specimens that had been used in a round robin.[8] It had been made by chemical vapor deposition (CVD). Details of the specimen preparation are given in Ref. 8. However, it should be noted that at least 50 μm of material from the nucleation surface of the specimen had been removed by grinding and polishing in order to insure specimen homogeneity. Earlier work had shown that as grown specimens show a large thermal conductivity inhomogeneity with material at the growth surface having significantly higher thermal conductivity than material at the nucleation surface. The growth surface of the diamond had also been polished in order to decrease the large surface roughness typical of CVD diamond growth surfaces.

A circuit typical of the three omega thermal conductivity measurement method[1] was produced on the top surface of the specimen by conventional photolithography used for production of integrated circuits. The metal heating strip, which was made of aluminum, was typically 200–300 nm thick. The widths of the strips were measured on a microscope equipped with a calibrated split image viewer. The widths of the lines were significantly narrower than the nominal line widths in the photomask indicating that significant undercutting occurred during the etching procedure. The standard uncertainty in the line widths was approximately 0.5 μm which is based on measurements by two difference operators.

TABLE I. Specimen specifications.

Specimen	Substrate thickness (μm)	Film thickness (nm)	Heater length (mm)	Heater width (μm)	Resistance at 20 °C (Ω)	dR/dT $\Omega\,K^{-1}$
SiO_2 on Si	510	52.7±0.6	4.00	28.3±0.5	27.3±0.3	0.089±0.009
SiO_2 on Si	510	101±1	4.00	28.4±0.5	27.1±0.3	0.090±0.009
SiO_2 on Si	510	200±2	4.00	28.5±0.5	26.8±0.3	0.088±0.009
SiO_2 on Si	380	488±5	4.00	28.3±0.5	27.3±0.3	0.090±0.009
CVD diamond	536	⋯	2.00	12.8±0.5	19.8±0.2	0.053±0.006

IV. EXPERIMENT

The basic electrical configuration of the three omega thermal conductivity measurement method we have employed and the measurement procedure employed were similar to D. G. Cahill's.[1] However, we replaced a digital-to-analog converter (DAC) with a manually adjustable potentiometer because unwanted signals were transmitted by the DAC at high heating frequencies (>8 kHz). We used a digital lock-in amplifier that could detect $V_{3\omega}$ directly. The output of the internal oscillator of the lock-in amplifier supplied the power to the specimen circuit. A 10 Ω reference resistor in series with the specimen was used to calibrate the current, allowing us to calculate the resistance of the heater and the power generated in the heater.

Measurements were made in a commercial thermostatically controlled oven retrofitted with water cooling coils; water was supplied by a heater/refrigerator water circulator. The oven temperature was controlled by a commercial temperature controller; measurements were made at nominal temperatures of 20 and 60 °C. The water temperature was set to 7 °C to allow for temperature stabilization in the oven within a reasonable length of time at 20 °C. At 60 °C, the water circulator was shut off.

The ambient oven temperature was measured with a type T thermocouple in close proximity to the specimen, although a temperature readout is also available as part of the oven temperature controller; the two temperatures agreed to within 1 K. The temperature instability was less than 0.1 K. The standard uncertainty in the temperature was as provided by the thermocouple manufacturer which was 0.5 K or 0.4% for temperatures above 0 °C.

The specimen temperature was actually slightly higher than the oven ambient because of heating by the heater strip. The specimen temperature and the temperature coefficient of resistance were obtained by measuring the resistance of the specimen at oven ambients of 20 and 60 °C at two power levels. At a particular temperature setting, the resistance was plotted versus the input power and the linear extrapolation of resistance to zero power input was taken to be the resistance of the specimen at the ambient temperature of the oven. By assuming a constant temperature coefficient of resistance between 20 and 60 °C, we were able to obtain the actual temperature of the specimen from the resistance of the specimen during a measurement.

The measurements were conducted under computer control. The ac voltage applied to the specimen circuit was 4.5 V_{RMS} for the diamond specimen and 2.5 V_{RMS} for the SiO_2 on silicon specimens. The relative uncertainty in all voltage readings was 0.1%.

The three omega signals from SiO_2/Si films have been analyzed with Eq. (1) for the cases of a film in intimate contact with a substrate and a film on substrate with a thermal resistance in series with the film. The three omega signals from the diamond specimen were analyzed with Eq. (1) for all of the cases shown in Fig. 1. We analyzed the data using case (c) in order to investigate whether a thermal conductivity gradient could be detected in the specimen.

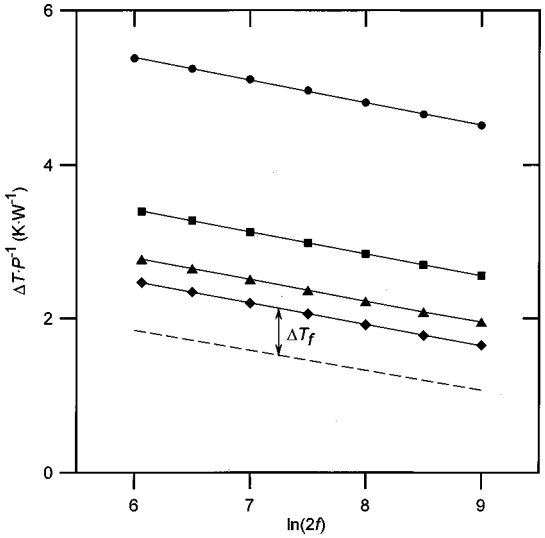

FIG. 2. The in-phase ac temperature of the metal strip as a function of heating frequency $(2f)$ for SiO_2 films on silicon substrates. ΔT_f represents the difference between the thermal signal for the coated substrate and the calculated thermal signal for a bare substrate. The solid lines are calculated based on fitting with the offset model. Within the resolution of the figure, curves calculated with the offset model cannot be distinguished from curves calculated with the two-layer model. The dashed line is the curve calculated for a bare silicon substrate of infinite thickness. The thicknesses of SiO_2 films are ● 488.3; ■ 200.4; ▲ 100.8; and ◆ 52.7 nm.

V. RESULT AND DISCUSSION

Figure 2 shows $\Delta T/P$ of the metal strip versus the heating frequency $(2f)$ for the set of SiO_2/Si films. The dots represent the experimental data, the solid lines represent fits to the experimental data, and the dashed line represents ΔT calculated for a bare silicon substrate based on a handbook value,[9] κ=1.52 W cm^{-1} K^{-1} at 21 °C. In the figure one observes that at given frequency, ΔT increases with increasing film thickness. Two models were used to fit the data but the results were indistinguishable within the resolution of the figure. One model is called the offset model.[2] It treats the film as a thermal resistance which results in an experimental curve that has the same shape as the curve calculated for uncoated silicon but is offset by an amount ΔT_f given by

$$\Delta T_f = \frac{P}{l\kappa_f}\frac{t}{2b}, \tag{6}$$

TABLE II. A comparison of the fitting results from the offset model, case (a) and two-layer model, case (b). The calibration temperature of specimen is about 21 °C. The handbook value of κ for silicon is[9] 1.52 W cm^{-1} K^{-1}.

Thickness of SiO_2 (nm)	Model	κ of Si (W cm^{-1} K^{-1})	κ of SiO_2 (W cm^{-1} K^{-1})
52.7±0.6	a	1.41±0.02	0.0089±0.0001
	b	1.41±0.02	0.0089±0.0001
101±1	a	1.40±0.02	0.0108±0.0001
	b	1.40±0.02	0.0107±0.0001
200±2	a	1.37±0.02	0.0124±0.0001
	b	1.38±0.01	0.0123±0.0001
488±5	a	1.33±0.02	0.0129±0.0001
	b	1.35±0.02	0.0127±0.0001

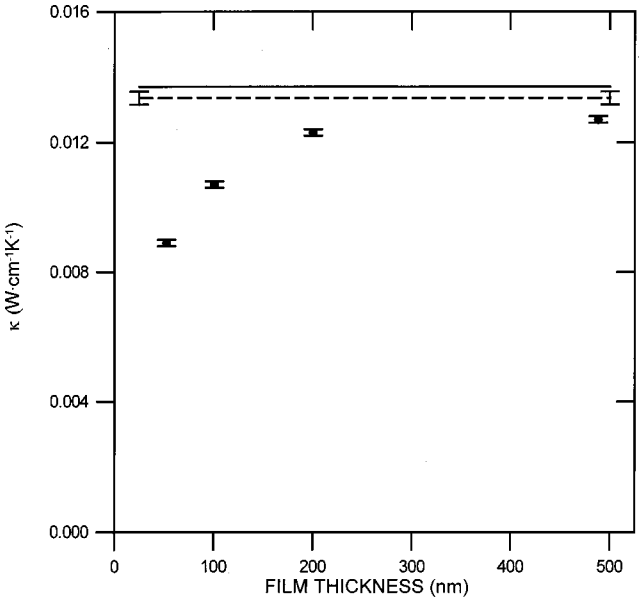

FIG. 3. The thermal conductivity of SiO_2 films as a function of thickness. Also shown is the thermal conductivity obtained (dashed line) if a constant thermal interface resistance is considered to exist either between the heater and the film and/or between the film and the substrate. For comparison, the handbook value for bulk SiO_2 (solid line) is also shown.

where t and κ_f are the thickness and thermal conductivity of thin film. However, the offset model usually considers the substrate to be infinitely thick. The second model is based on case (b) of Fig. 1. Table II shows the results of the two models. The good agreement of the two models occurs because the substrate is thicker than the longest thermal diffusion length, which occurs at the lowest modulation frequency. Values of κ for the silicon substrate were obtained as well. These values agree reasonably well with the handbook value.[9]

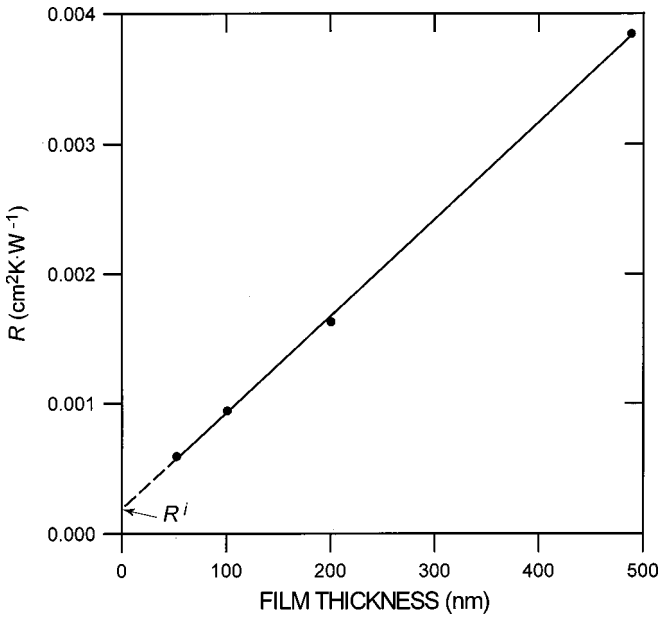

FIG. 4. Plot of the thin film thermal resistance of the SiO_2 films as a function of thickness. The straight-line behavior suggests that the thermal conductivity can be considered independent of thickness. The nonzero intercept, R^i, represents a fixed thermal resistance present in all of the specimens.

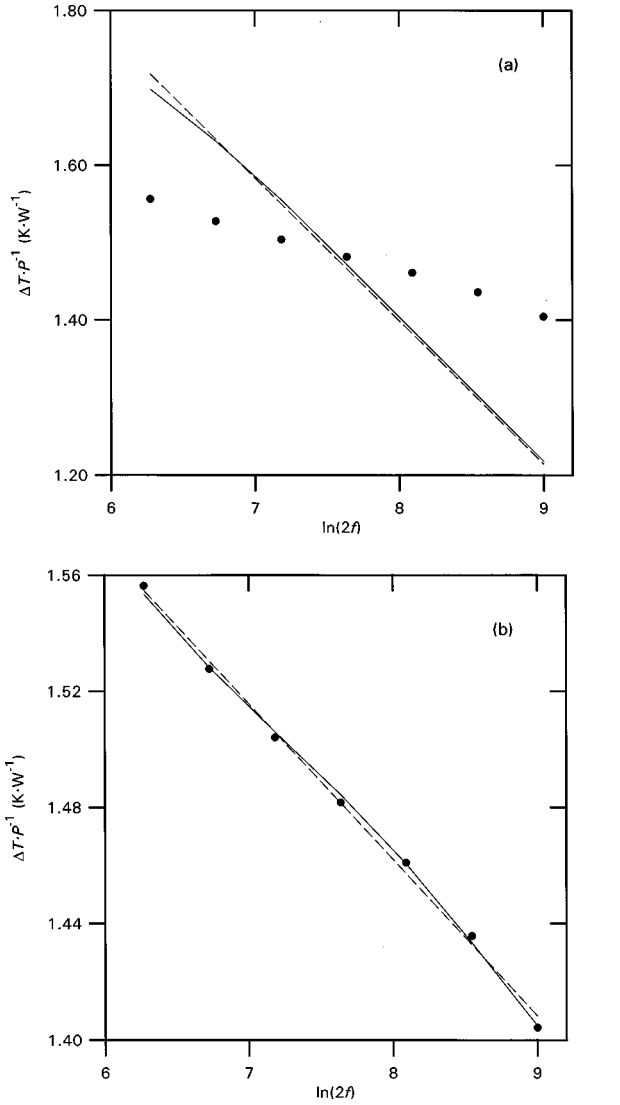

FIG. 5. The in-phase ac temperature of the metal strip as a function of heating frequency for CVD diamond. The points represent the experimental data. (a) The dashed line is the fit for a semi-infinite solid; the solid line is the fit for a solid of finite thickness. (b) The dashed line is the fit for the offset model; the solid line is the fit for the two-layer model. The two-layer model gives the best fit.

The black dots in Fig. 3 show the thin film thermal conductivity κ_f as a function of film thickness for SiO_2 films on Si based on the model in Fig. 1(a). The handbook value for silica,[9], $\kappa=0.0137\ \mathrm{W\,cm^{-1}\,K^{-1}}$ is given by the solid line. Generally, κ_f of every film appears to be lower than κ of bulk SiO_2. Furthermore, κ_f is seen to decrease with a decreasing thickness. This might indeed be the case; however, there is an alternate explanation for these results. Figure 4 shows a plot the thermal resistance of the films, $R=L/\kappa_f$ as a function of film thickness, L. The straight-line behavior suggests that the thermal conductivity is independent of L; the apparent decrease in κ_f with decreasing L could be due to a thermal resistance layer within the specimen structure. If we fit a straight line through the experimental points, the

TABLE III. Comparison between multilayer models for the diamond specimen. The measurement temperature is 27.7 °C. κ_j refers to the thermal conductivity of the jth layer and R_k^i represents the thermal resistance of the kth layer. The round robin gave $\kappa = 12.92\ \mathrm{W\,cm^{-1}\,K^{-1}}$ at 25 °C. The units of κ_j are $\mathrm{W\,cm^{-1}\,K^{-1}}$ and the units of R_j^i are $\mathrm{cm^2\,K\,W^{-1}}$

Case a	Case b	Case c
$R_2^i = 2.5 \times 10^{-4}$	$R_2^i = 2.4 \times 10^{-4}$	$R_3^i = 2.4 \times 10^{-4}$
$\kappa_1 = 14.8 \pm 0.4$	$\kappa_1 = 12.9 \pm 0.3$	$\kappa_2 = 13.0 \pm 0.6$
		$\kappa_1 = 11 \pm 6$

slope gives the reciprocal thickness-independent thermal conductivity, κ^{-1}, and the intercept represents an interfacial thermal resistance, $R^i = 1.8 \times 10^{-4}\ \mathrm{cm^2\,K\,W^{-1}}$. We cannot tell whether R^i is between the film and the substrate or between the heater and the film. However, the value we obtain for R^i is comparable to the value obtained by S. M. Lee[3] and D. G. Cahill ($R \sim 2 \times 10^{-4}\ \mathrm{cm^2\,K\,W^{-1}}$) in other film/substrate systems. The dashed line in Fig. 3 shows the value of the thickness-independent κ calculated from the R vs L plot.

Figure 5 shows $\Delta T/P$ vs $\ln(2f)$ for the diamond specimen. The solid dots represent the experimental data. The lines represent different theoretical fits to the experimental data. In Fig. 5(a), the lines represent fits to the data that assume no interface layer between the heater and the specimen. The dashed line assumes that the thickness of the specimen can be ignored ($L = \infty$) whereas the solid line takes into account the finite thickness of the specimen. There is a small yet noticeable difference between the two lines; however, the fits to the data are poor. The poor fit is the due to the size of the signal which is higher than would be expected if κ had been calculated only from the average slope of the data. The theoretically expected curve would be offset downward from the measured curve by an approximately constant amount. An interfacial thermal resistance could account for such an offset.

Thus, Fig. 5(b) shows fits that include an interfacial layer between the heater and the substrate. The dashed curve was calculated with the offset model which is based on the configuration of Fig. 1(a). The solid curve is based on Fig. 1(b) which assumes a substrate of finite thickness; we call this the two-layer model. Both models show a much better fit than the models depicted in Fig. 1(a). However, the model that assumes a finite substrate thickness does fit the data better than the model that assumes infinite substrate thickness. This is because the thermal diffusion length in the fitting range is greater than the specimen thickness. The fit was accomplished by fixing the interfacial film thickness and calculating the best values of κ. We found that the ratio L/κ was independent of the chosen film thickness provided L was chosen sufficiently small ($L < 1\ \mu\mathrm{m}$). Thus, this interfacial layer is equivalent to a thermal resistance, R^i.

Values of κ and R^i for each of the models used to fit the diamond data are shown in Table III; in the table, a subscript on κ and R^i denotes the layer to which the value applies. The values of R^i appear to be model independent and are very close to the value calculated for the SiO_2/Si films reported earlier and to the value reported in the literature.[3]

In addition to the previously discussed models, we have considered the model depicted in Fig. 1(c). As-grown CVD diamond is known to have a thermal conductivity gradient through the thickness.[10] A simple way of detecting such a gradient would be to fit the experimental data with a model that divides the diamond into two layers of equal thickness and then to calculate κ of each layer. A gradient should yield different values of κ for each layer. An examination of the results of this model shows no statistically significant difference between κ of the two diamond layers. However, the mean values show the trend that would be expected; the value of the layer containing the growth surface is higher than the layer containing the surface closest to the nucleation surface. As mentioned earlier, the nucleation surface had been removed to improve the homogeneity of the specimen.

We conclude that the model of Fig. 1(b) provides the best fit to the CVD diamond data. There are several possible explanations for an interfacial layer. Surface contamination of the specimen can lead to a lack of intimate adhesion of the deposited metal film used for the heater strip. In the case of CVD diamond, a graphitic layer between the heater and the diamond is also possible. In addition, a Nomarski micrograph reveals an uneven surface containing stepped artifacts that had not been removed by the polishing procedure. Thus, the residual surface roughness may also contribute to the interfacial thermal resistance.

In conclusion, we have successfully applied multilayer models to analyze data obtained by the three omega thermal conductivity measurement method. The thermal conductivities of high and low κ materials can be obtained.

ACKNOWLEDGMENTS

The authors thank David Cahill for helpful advice in implementing the three omega thermal conductivity measurement method. Dr. Kim acknowledges stimulating conversations with Dr. Do-Kyung Kim regarding thermal conductivity measurement. Dr. Kim would also like to thank Bev Anderson for editing the initial draft of the manuscript. Dr Kim received most of his support from the Korea Science and Engineering Foundation with supplementary support from NIST.

[1] D. G. Cahill, Rev. Sci. Instrum. **61**, 802 (1990).
[2] D. G. Cahill, M. Katiyar, and J. R. Abelson, Phys. Rev. B **50**, 6077 (1994).
[3] S.-M. Lee and D. G. Cahill, J. Appl. Phys. **81**, 2590 (1997).
[4] N. O. Birge, Phys. Rev. B **34**, 1631 (1986).
[5] D. G. Cahill and R. O. Pohl, Phys. Rev. B **35**, 4067 (1986).
[6] A. Feldman, NISTIR 5928 (1996); A. Feldman, High-Temperatures High-Pressures **31**, 293 (1999).
[7] H. S. Carslaw and J. C. Jaeger, *Conduction of Heat in Solids* (Oxford University Press, London, 1959), p. 111.
[8] J. E. Graebner *et al.*, Diamond Relat. Mater. **7**, 1589 (1998).
[9] Y. S. Touloukian, R. W. Powel, C. Y. Ho, and P. G. Klemens, *Thermal Conductivity* TPRC Data series, Vol. 1 (IFI/Plenum, New York, 1970).
[10] J. E. Graebner, S. Jin, G. W. Kammlott, Y.-H. Wong, J. A. Herb, and C. F. Gardinier, Diamond Relat. Mater. **2**, 1059 (1993).